ChemComm

COMMUNICATION

View Article Online
View Journal | View Issue

Cite this: *Chem. Commun.*, 2021, **57**, 11645

Received 14th September 2021,
Accepted 13th October 2021

DOI: 10.1039/d1cc05193h

rsc.li/chemcomm

Stable pseudo[3]rotaxanes with strong positive binding cooperativity based on shape-persistent aromatic oligoamide macrocycles†‡

Thomas A. Sobiech,§[a] Yulong Zhong,§[a] Laura S. Sánchez B.,[b] Brice Kauffmann,[c] Jillian K. McGrath,[a] Christina Scalzo,[a] Daniel P. Miller,[b] Ivan Huc,[d] Eva Zurek,[a] Yann Ferrand[c] and Bing Gong*[a]

New aromatic oligoamide macrocycles with C_3-symmetry bind a bipyridinium guest (G) to form compact pseudo[3]rotaxanes involving interesting enthalpic and entropic contributions. The observed high stabilities and strong positive binding cooperativity are found in few other host–guest systems.

Shape-persistent molecular architectures have attracted significant scientific interest, as their defined structural characteristics provide unique opportunities for both basic understanding and practical applications.[1] Compared to flexible structures, shape-persistent molecules offer distinctive advantages. Such molecules, with their discrete sizes and defined shapes, engage in predictable intermolecular association and assembly as a result of the cooperative and controlled action of multiple non-covalent forces. By minimizing the energy cost associated with conformational changes, shape-persistent foldamers[2] and macrocycles[3] are able to rigidly hold and convergently orient binding sites, based on which hosts containing preorganized cavities with extraordinary guest-binding capabilities are created.

Over the years, we have discovered and studied the six-residue aromatic amide macrocycle **1** and its analogs.[4] Macrocycle **1** has a persistent shape with its backbone being fully constrained due to the presence of highly favorable, three-center intramolecular hydrogen bonds.[5] The internal cavity of **1**, being decorated with six rigidly held amide carbonyl groups that orient toward the center of the macrocycle, is electronegative and capable of strongly binding cationic guests. For example, the guanidinium ion has been found to bind tightly with **1**.[6] Guests based on bipyridinium derivatives have been found to form 2 : 1 (host : guest) complexes with **1**.[7] Macrocycle **1** is equipped with proper side-chains stacked into membrane-spanning columnar assemblies with electronegative cylindrical inner pores, which serve as highly conducting channels for cations.[8]

Consisting of alternating diacid and diamine residues derived from the corresponding *meta*-disubstituted benzene derivatives, macrocycle **1** is one of many possible types of aromatic oligoamide macrocycles that have constrained backbones. Macrocycles of various sizes that have the same backbone as **1** have been constructed.[9] However, adjusting the orientations of the amide groups of the backbone should lead to new macrocycles that have persistent shapes but with altered backbones and cavities containing various arrangements of amide oxygen atoms. For example, inverting the orientation of every second amide group in the backbone of **1** results in macrocycle **2**, which has remained unknown until now (Fig. 1).

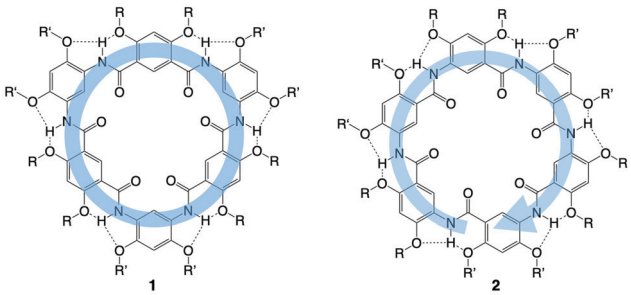

Fig. 1 Inverting the orientation of every second amide group in the backbone of macrocycle **1**, which has a C_2- and C_3-symmetrical backbone highlighted with a blue circle, results in macrocycle **2**, which has a C_3-symmetrica (*N*-to-*C*) backbone highlighted with a circular, blue arrow. Hydrogen bonds are shown as dashed lines. R and R′ are methyl groups and other side-chains.

[a] *Department of Chemistry, University at Buffalo, the State University of New York, Buffalo, New York 14260, USA. E-mail: bgong@buffalo.edu*
[b] *Department of Chemistry 151 Hofstra University 106F Berliner Hall Hempstead, NY 11549, USA*
[c] *Institut Européen de Chimie et Biologie, UMS3011/US001 CNRS, Inserm, Université de Bordeaux, 2 rue Robert Escarpit, F-33600 Pessac, France*
[d] *Department Pharmazie, Ludwig-Maximilians-Universität München, Butenandtstraße 5-13, D-81377 Munich, Germany*

† This work is dedicated to Professor David G. Lynn in celebration of his 70th birthday.

‡ Electronic supplementary information (ESI) available. CCDC 2103074. For ESI and crystallographic data in CIF or other electronic format see DOI: 10.1039/d1cc05193h

§ These authors contributed equally to this work.

Like **1**, macrocycle **2** has an aromatic oligoamide backbone that is fully constrained due to the presence of three-center intramolecular hydrogen bonds. Unlike **1**, macrocycle **2** consists of basic residues that share the same core based on 5-amino-2,4-dialkoxybenzoic acid and thus have the same electronic properties. In contrast to macrocycle **1**, which has D_3-symmetry, macrocycle **2** has C_3-symmetry and a backbone with a circular *N*-to-*C*, *i.e.*, clockwise or counterclockwise, direction. With a backbone that is electronically different from that of **1**, macrocycle **2** is expected to have different assembly properties. Furthermore, the cavity of **2** differs from that of **1** by having convergently oriented, equidistant amide oxygen atoms, which could lead to distinctive guest-binding behavior.

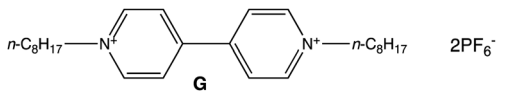

G

Herein, we report the synthesis, guest-dependent discrete assembly, and guest-binding behavior of **2**. Guest **G**, derived from the alkylation of 4,4′-bipyridine with *n*-octyl bromide, followed by exchanging Br^- with PF_6^- ions, was chosen to examine the capability of **2** in binding cationic species. This is because similar bipyridinium guests have been widely used in assessing the binding capabilities of hosts with electronegative cavities.[10,11]

Our studies revealed that macrocycle **2** bound **G** strongly, with an overall binding constant of over 10^{11} M^{-2} and a 2 : 1 stoichiometry in the polar solvent DMSO/$CHCl_3$ (1/1, v/v). The formation of the 2 : 1 complexes, as highly stable pseudo[3]rotaxanes,[12] shows very strong positive cooperativity, with the second binding even being much more favorable than the first one. The X-ray structure reveals a highly compact pseudo[3]rotaxane in which two molecules of **2** undergo strong aromatic stacking with their backbones following the same *N*-to-*C* direction, *i.e.*, clockwise or counterclockwise Scheme 1.

Macrocycles **2a** and **2b** were synthesized from noncyclic **3a** and **3b**, which are members of aromatic oligoamide foldamers that we developed over the years.[13] Removing the CBZ and *t*-butyl groups from oligoamides **3a** and **3b** gave amine- and carboxyl-terminated hexamers, which, with constrained backbones enforcing stably folded, crescent conformations, were predisposed to cyclization. Macrocycles **2a** and **2b** were obtained in good to excellent isolated yields (from 43% to 80%) by treating the corresponding linear hexamers with the coupling reagent 1-[bis(dimethylamino)methylene]-1*H*-1,2,3-triazolo[4,5-*b*]pyridinium 3-oxide hexafluorophosphate (HATU).

The proton resonances of **2a** (1 mM) appear as featureless broad peaks in $CDCl_3$, suggesting self-aggregation that restricts the motion of the macrocyclic molecules. Adding DMSO-d_6 to $CDCl_3$ resulted in the sharpening and downfield shifting of ^{1}H NMR signals, with the ^{1}H NMR peaks becoming well dispersed upon increasing the ratio of DMSO-d_6 to 20% (by volume) or more. The NMR signals continued to sharpen and shift downfield with increasing DMSO-d_6 ratio, indicating the weakening of aggregation and aromatic stacking interactions in solvents of enhanced polarity (Fig. S1, ESI‡). With 50% (by volume) or more of DMSO-d_6 in $CDCl_3$, the line width of the NMR peaks ceased to change, which points to the complete interruption of aggregation. In DMSO-d_6/$CDCl_3$ (1/1, v/v), the ^{1}H NMR resonances of **2a** from 1 mM to 0.05 mM remained unchanged in both their line widths and chemical shifts (Fig. S2, ESI‡), demonstrating that **2a** became molecularly dissolved.

Examining the mixture of **2a** or **2b** and **G** with Electrospray-ionisation quadrupole time-of-flight mass spectrometry (ESI-Q-TOF) revealed ions with mass/charge ratios at 1867.0657 and 2058.9883, respectively, which appear as base peaks in the mass spectra (Fig. S3, ESI‡). These peaks correspond to the 2 : 1 complexes of **2a** and **2b** with **G**, *i.e.*, pseudo[3]rotaxanes, as confirmed by the excellent match of the measured and simulated isotope distributions (Fig. 2). Ions corresponding to the 1 : 1 complexes of **2a** and **2b** with **G**, with mass/charge ratios of 1029.1089 and 1125.0772, respectively, only appear as minor peaks in the mass spectra (Fig. S3, ESI‡). These results indicate that **2a** and **2b** bind **G** strongly in a 2 : 1 stoichiometry. The fact that the ions corresponding to the 2 : 1 complexes give rise to the most prominent peaks in the mass spectra demonstrates the high stabilities of the pseudo[3]rotaxanes.

Mixing the solutions of **2a** and **G**, both colorless, gave a solution that turned light yellow. This observation prompted us to examine the binding of **2a** with **G** by performing UV-vis titration in DMSO/$CHCl_3$ (1/1, v/v) (Fig. S4, ESI).‡ Plotting the change in the absorbance of **2a** (1 mM) at 430 nm against the proportion of **G** (0 to 2 equiv.) revealed two distinct trend lines showing an abrupt change in their slopes at ~0.5 equiv. of **G** (Fig. S4, ESI‡). This confirms the 2 : 1 binding of **2a** and **G** revealed by the ESI-Q-TOF results. The abrupt change indicates a proper titration regime at the concentrations used in this

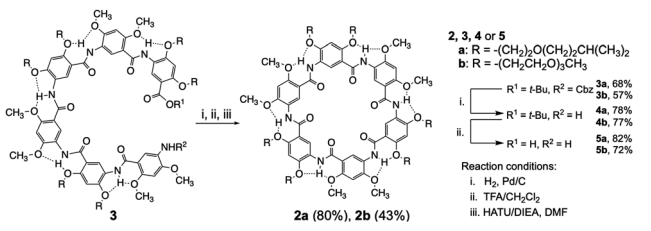

Scheme 1 Synthesis of macrocycles **2a** and **2b**.

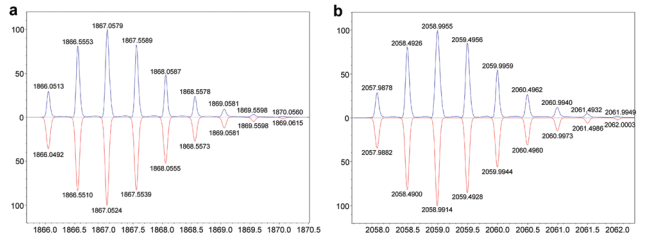

Fig. 2 Isotope distributions of (a) [**2a** + **G** + **2a**]$^{2+}$ and (b) [**2b** + **G** + **2b**]$^{2+}$ ions from ESI-Q-TOF (blue) and computer simulation (red).

Table 1 Thermodynamic parameters, binding constants and interaction parameters (α) for the 2 : 1 complexes of hosts **2a** and **2b** with guest **G**[a]

	2a	**2b**
ΔH_1 (cal mol^{-1})	$(-1.94 \pm 0.31) \times 10^3$	$(5.97 \pm 2.29) \times 10^3$
$T\Delta S_1$ (cal mol^{-1})	$(5.18 \pm 2.21) \times 10^3$	$(12.5 \pm 2.87) \times 10^3$
K_1 (M^{-1})	$(1.69 \pm 0.52) \times 10^5$	$(6.41 \pm 1.70) \times 10^4$
ΔH_2 (cal mol^{-1})	$(-5.16 \pm 0.29) \times 10^3$	$(-14.7 \pm 2.30) \times 10^3$
$T\Delta S_2$ (cal mol^{-1})	$(3.37 \pm 2.07) \times 10^3$	$(-6.31 \pm 3.14) \times 10^3$
K_2 (M^{-1})	$(1.79 \pm 0.43) \times 10^6$	$(1.47 \pm 0.38) \times 10^6$
K_{total} (M^{-2})	$(3.03 \pm 1.18) \times 10^{11}$	$(9.42 \pm 3.49) \times 10^{10}$
α[b]	42	92

[a] The data here are a summary of binding data obtained from ITC titrations of **2a** (450 μM) or **2b** (450 μM) into **G** (25 μM) in DMSO/$CHCl_3$ (1/1, v/v) at 25 °C. [b] The interaction parameter $\alpha = 4K_2/K_1$ ($\alpha > 1$: positive cooperativity; $\alpha < 1$: negative cooperativity; $\alpha = 1$: no cooperativity).[14]

experiment. Thus, efforts to fit the UV-vis titration data failed to yield satisfactory results due to large errors.

To gain additional insights into the host–guest interaction between macrocycle **2** and guest **G**, the affinities of **2a** and **2b** for **G**, along with other thermodynamic parameters of the binding events, were determined with isothermal titration calorimetry (ITC) experiments. In DMSO/$CHCl_3$ (1/1, v/v), both **2a** and **2b** bind **G** in high binding affinities, with the overall binding constants being around 10^{11} M^{-2} (Table 1).

The stepwise binding constants K_1 and K_2, along with the corresponding enthalpy and entropy changes, reveal interesting similarities and differences between the two host–guest pairs (Table 1 and Fig. S5, ESI‡). Differing only in their side-chains, macrocycles **2a** and **2b** show different details in their binding of **G**. For both complexes, the first and second binding events are entropically and enthalpically driven, respectively. The first binding events of **2a** and **2b** with **G**, being both entropically dominant, involve opposite enthalpic contributions. That of **2a** is enthalpically favorable and that of **2b** is unfavorable. In contrast, the second binding events of **2a** and **2b** with **G**, being both enthalpically dominant, involve opposite entropic contributions. That of **2a** is entropically favorable and that of **2b** is unfavorable. The observed differences in the behavior of **2a** and **2b** may be due to different solvation of these two macrocycles. The differences in their side-chains may lead to different enthalpic and entropic outcomes. The specific factors responsible for the observed differences remain to be elucidated, and will require additional systematic studies.

For both complexes, the K_2 values are 10 to 20 times greater than the K_1 values. Thus, for **2a** or **2b**, the second molecule binds to **G** in much higher affinity than the first one does. As indicated by the interaction parameters (α) of 42 and 92[14] for **2a** and **2b**, respectively, the formation of the pseudo[3]rotaxanes involves fairly strong positive cooperativity.

Unlike that of **1**, the oligoamide backbone of **2a** and **2b** seems to have a higher propensity for intermacrocyclic stacking interactions, which, along with electrostatic and perhaps C–H···O hydrogen-bonding interactions between the host and guest, promotes the binding of the second macrocycle and the positive cooperativity in the binding of **G** to **2a** or **2b**.

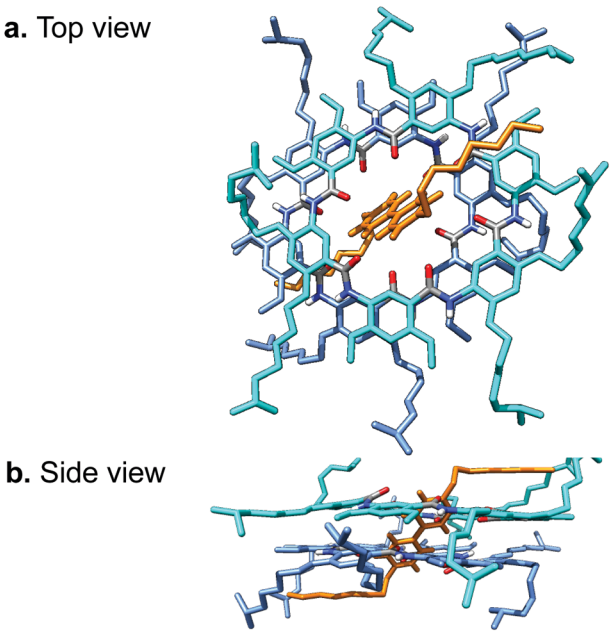

Fig. 3 Crystal structure of pseuo[3]rotaxane $\mathbf{2a_2}$·**G**. PF_6^- ions and hydrogen atoms, except for those of the bipyridinium unit of **G** and the amide groups of **2a**, are omitted. Amide groups are shown by element color to indicate backbone orientation. **G** is shown in orange. The two molecules of **2a** are shown in cyan and cornflower blue, respectively.

Single crystals, obtained by slow liquid–liquid diffusion of CH_3OH into a solution of **2a** and **G** in CH_2Cl_2, provided the crystal structure of pseudo[3]rotaxane $\mathbf{2a_2}$·**G** (Fig. 3). Guest **G** threads through the 8.2 Å (or 5.1 Å vdw) cavities of the macrocycles, with the long axis of its bipyridinium unit being tilted at an angle of ~45° to the C_3 axis of symmetry of each macrocycle. The bipyridinium CH groups engage in C–H···O interactions, with each of the pyridinium rings forming C–H···O bonds with four of the six amide O atoms of each macrocycle.

N^+···O distances of 3.23 Å and 3.46 Å were found between each of the pyridinium N atoms and two amide O atoms of one of the two macrocycles, indicative of strong charge-dipole interactions. The two octyl ''tails'' of **G** are within van der Waals contact distances of an aromatic residue from one of the two macrocycles, which cap the dimeric stack of **2a** (Fig. 3b).

In addition to the observed interactions between **2a** and **G**, the two macrocycles in the pseudo[3]rotaxane adopt nearly planar conformations and are in close contact, with intermacrocyclic stacking distances between 3.4 and 3.5 Å, indicating very strong stacking interactions. The two macrocycles in $\mathbf{2a_2}$·**G** are offset and have their backbone in the same clockwise (or counterclockwise) *N*-to-*C* direction. The other possible arrangement of the two macrocycles, one with its backbone being in a clockwise and the other in a counterclockwise direction, is absent in the X-ray structure.

Thus, the X-ray structure reveals the atomic details of a compact complex of **2a** and **G** in which the bipyridinium segment of guest **G** is completely encapsulated in the cavities

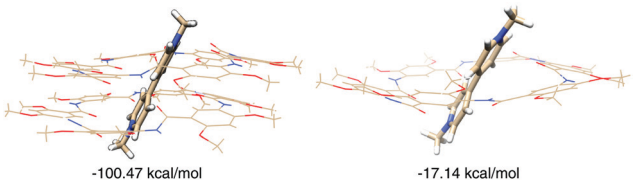

Fig. 4 Energy-minimized structures of the 2 : 1 complex $\mathbf{2_2}$·**G** (left) and 1 : 1 complex **2**·**G** (right) DMSO/$CHCl_3$ (1/1, v/v). The octyl end groups of guest **G** and the R side-chains of **2** are replaced with methyl groups in the computed structures. Interaction energies ESI‡ are shown underneath the structures.

of two stacked molecules of **2a**. Along with the van der Waals contacts between the octyl end groups and the backbone aromatic residues of **2a**, this structure results in maximum contact between **2a** and **G**. Strong stacking between the two molecules of **2a** provides additional stabilization for the complex, leading to the strong cooperativity observed in the binding of **2** and **G**.

The interaction parameters (α) of 42 and 92 observed with the binding of **2a** or **2b** with **G** reveal strong positive cooperativity. In contrast, the binding of macrocycle **1** with bipyridinium guests showed negative to weakly positive cooperativity with the largest α value being 2.5.[7] This noticeable cooperativity was probed by performing density functional theory calculations on the binding of **2** with **G**.[15] The optimized structure of complex $\mathbf{2_2}$·**G** (Fig. 4, left) closely resembles the crystal structure of $\mathbf{2a_2}$·**G**, indicating the reliability of our method. The interaction energy ESI,‡ which reflects the binding between **2** and **G**, of complex $\mathbf{2_2}$·**G** is much larger in magnitude than that of binding one molecule of **2** to **G** (Fig. 4, right). These results show that the second binding event is energetically highly favorable, which is in line with the experimentally observed strong positive cooperativity in the binding of **G** with **2**.

In summary, macrocycles **2a** and **2b** were found to strongly bind to bipyridinium guest **G** in a 2 : 1 stoichiometry, forming highly stable pseudo[3]rotaxanes. Results from ITC titrations reveal that the interaction of **2** with **G** features strong overall binding, different dominant entropic or enthalpic factors associated with the first and second binding events, and, most prominently, much stronger positive cooperativities than those observed with other aromatic oligoamide macrocycles of comparable sizes. The X-ray structure of pseudorotaxane $\mathbf{2a_2}$·**G** reveals a compact assembly that is stabilized by hydrogen-bonding, charge-dipole, aromatic stacking, and van der Waals interactions. Computational studies reveal a drastically enhanced interaction for the 2 : 1 complex over that of the 1 : 1 complex, which further demonstrates the strong positive cooperativity of this system. Macrocycle **2** represents a new member of aromatic oligoamide macrocycles, based on which highly stable pseudorotaxanes are being developed.

Synthesis and characterization (T. A. S., Y. L. Z., J. K. M., C. S.); computation (L. S. S. B., D. P. M., E. Z.); X-ray crystallography (B. K., Y. F., I. H.); general discussion (T. A. S., Y. L. Z., D. P. M., I. H., E. Z., Y. F., B. G.); design and manuscript writing (B. G.).

This research was supported by the American Chemical Society-Petroleum Research Fund (PRF No. 58364-ND7 to B. G.), and the US National Science Foundation (CHE-1905094 and 2108538 to B. G. and CHE-2108597 to D. P. M.).

Conflicts of interest

There are no conflicts to declare.

Notes and references

1 (*a*) J. L. Sessler and A. K. Burrell, *Top. Curr. Chem.*, 1992, **161**, 177; (*b*) J. S. Moore, *Acc. Chem. Res.*, 1997, **10**, 402; (*c*) B. Gong, *Chem. – Eur. J.*, 2001, **7**, 4336; (*d*) S. Höger, *Chem. – Eur. J.*, 2004, **10**, 1320; (*e*) H. Juwarker and K.-S. Jeong, *Chem. Soc. Rev.*, 2010, **39**, 3664; (*f*) K. P. McDonald, Y. R. Hua, S. Lee and A. H. Flood, *Chem. Commun.*, 2012, **48**, 5065; (*g*) T. Ogoshi, T.-A. Yamagishi and Y. Nakamoto, *Chem. Rev.*, 2016, **116**, 7937.

2 (*a*) J. Zhu, R. D. Parra, H. Q. Zeng, E. Skrzypczak-Jankun, S. Martinovic, X. C. Zeng and B. Gong, *J. Am. Chem. Soc.*, 2000, **122**, 4219; (*b*) H. Jiang, J.-M. Léger and I. Huc, *J. Am. Chem. Soc.*, 2003, **125**, 3448; (*c*) J.-L. Hou, X.-B. Shao, G.-J. Chen, Y.-X. Zhou, X.-K. Jiang and Z.-T. Li, *J. Am. Chem. Soc.*, 2004, **126**(39), 12386; (*d*) K. J. Chang, B. N. Kang, M. H. Lee and K.-S. Jeong, *J. Am. Chem. Soc.*, 2005, **127**, 12214; (*e*) Y. Yan, B. Qin, C. L. Ren, X. Y. Chen, Y. K. Yip, R. J. Ye, D. W. Zhang, H. B. Su and H. Q. Zeng, *J. Am. Chem. Soc.*, 2010, **132**, 5869; (*f*) Y. R. Hua, Y. Liu, C. H. Chen and A. H. Flood, *J. Am. Chem. Soc.*, 2013, **135**, 14401; (*g*) C. J. Massena, N. B. Wageling, D. A. Decato, E. M. Rodriguez, A. M. Rose and O. B. Berryman, *Angew. Chem., Int. Ed.*, 2016, **55**, 12398.

3 (*a*) J. L. Sessler, S. J. Weghorn, T. Morishima, M. Rosingana, V. Lynch and V. Lee, *J. Am. Chem. Soc.*, 1992, **114**, 8306; (*b*) K. H. Choi and A. D. Hamilton, *J. Am. Chem. Soc.*, 2001, **123**, 2456; (*c*) L. He, Y. An, L. H. Yuan, W. Feng, M. F. Li, D. C. Zhang, K. Yamato, C. Zheng, X. C. Zeng and B. Gong, *Proc. Natl. Acad. Sci. U. S. A.*, 2006, **103**, 10850; (*d*) S. J. Brooks, P. A. Gale and M. E. Light, *Chem. Commun.*, 2006, 4344; (*e*) H. L. Fu, Y. Liu and H. Q. Zeng, *Chem. Commun.*, 2013, **49**, 4127; (*f*) J. H. Oh, J. H. Kim, D. S. Kim, H. J. Han, V. M. Lynch, J. L. Sessler and S. K. Kim, *Org. Lett.*, 2019, **21**, 4336.

4 L. H. Yuan, W. Feng, K. Yamato, A. R. Sanford, D. G. Xu, H. Guo and B. Gong, *J. Am. Chem. Soc.*, 2004, **126**, 11120.

5 R. D. Parra, H. Q. Zeng, J. Zhu, C. Zheng, X. C. Zeng and B. Gong, *Chem. – Eur. J.*, 2001, **7**, 4352.

6 A. R. Sanford, L. H. Yuan, W. Feng, K. Yamato, R. A. Flowers and B. Gong, *Chem. Commun.*, 2005, 4720.

7 X. W. Li, X. Y. Yuan, P. C. Deng, L. X. Chen, Y. Ren, C. Y. Wang, L. X. Wu, W. Feng, B. Gong and L. H. Yuan, *Chem. Sci.*, 2017, **8**, 2091.

8 A. J. Helsel, A. L. Brown, K. Yamato, W. Feng, L. H. Yuan, A. Clements, S. V. Harding, G. Szabo, Z. F. Shao and B. Gong, *J. Am. Chem. Soc.*, 2008, **130**, 15784.

9 W. Feng, L. Yamato, L. Q. Yang, J. Ferguson, L. J. Zhong, S. L. Zou, L. H. Yuan, X. C. Zeng and B. Gong, *J. Am. Chem. Soc.*, 2009, **131**, 2629.

10 (*a*) M. M. Zhang, K. L. Zhu and F. H. Huang, *Chem. Commun.*, 2010, **46**, 8131; (*b*) A. Trabolsi, *Nat. Rev. Chem.*, 2021, **5**, 442.

11 (*a*) W. Ong, M. Gómez-Kaifer and A. E. Kaifer, *Org. Lett.*, 2002, **4**, 1791; (*b*) K. Moon and E. Kaifer, *Org. Lett.*, 2004, **6**, 185; (*c*) T. Ogoshi, M. Hashizume, T. Yamagishi and Y. Nakamoto, *Chem. Commun.*, 2010, **46**, 3708; (*d*) N. K. Beyeh, H. H. Jo, I. Kolesnichenko, F. Pan, E. Kalenius, E. V. Anslyn, R. H. A. Ras and K. Rissanen, *J. Org. Chem.*, 2017, **82**, 5198.

12 M. Xue, Y. Yang, X. D. Chi, X. Z. Yan and F. H. Huang, *Chem. Rev.*, 2015, **115**, 7398.

13 L. H. Yuan, A. R. Sanford, W. Feng, A. M. Zhang, J. S. Ferguson, K. Yamato, J. Zhu, H. Q. Zeng and B. Gong, *J. Org. Chem.*, 2005, **70**, 10660.

14 (*a*) K. A. Connors, A. Paulson and D. Toledo-Velasquez, *J. Org. Chem.*, 1988, **53**, 2023; (*b*) C. A. Hunter and H. L. Anderson, What is cooperativity?, *Angew. Chem., Int. Ed.*, 2009, **48**, 7488; (*c*) P. Thordarson, *Chem. Soc. Rev.*, 2011, **40**, 1305.

15 G. te Velde, F. M. Bickelhaupt, E. J. Baerends, C. Fonseca Guerra, S. J. A. van Gisbergen, J. G. Snijders and T. Ziegler, *J. Comput. Chem.*, 2001, **22**, 931.

